

June 2014

Histone Deacetylase Inhibitors: Role in Gene Expression and Development of New Anticancer Drug Candidates

Mohamed Ammar
mohhayammar@gmail.com

Follow this and additional works at: https://opencommons.uconn.edu/srhonors_theses

Recommended Citation

Ammar, Mohamed, "Histone Deacetylase Inhibitors: Role in Gene Expression and Development of New Anticancer Drug Candidates" (2014). *Honors Scholar Theses*. 351.
https://opencommons.uconn.edu/srhonors_theses/351

Histone Deacetylase Inhibitors: Role in Gene Expression and Development of New Anticancer Drug Candidates

Mohamed Ammar

Abstract:

Histone deacetylase (HDAC) suppresses gene expression by removing acetyl groups from lysine residues in chromatin. Inhibitors play an important role by restoring the ability of the gene to be expressed, which is crucial if the gene is a tumor suppressor gene. HDACs consist of four classes, spanning 18 isozymes. Current HDAC inhibitors approved and in development are considered pan-inhibitors, blocking a wide array of HDAC isozymes, increasing the risk of adverse effects. β -thujaplicin is derived from the heartwood of trees in the cupressaceae family and from it is derived the tropolone scaffold. The tropolone scaffold involves several advantages over other classes of HDAC inhibitors, such as various positions in which diverse functional groups can attach and thus can direct specificity to certain HDAC isozymes. Herein we describe our efforts to develop compounds at the α -position of the tropolone scaffold as well as preliminary biologic data.

Introduction:

In eukaryotic cells, DNA is contained in a condensed and tightly packed structure called chromatin. Structural modification of chromatin may occur by adding acetyl groups, which neutralize positively charged lysine residues in the chromatin. This causes the chromatin to become loosely packed and as a result permits the DNA to be accessible for gene transcription. Consequently, removing the acetyl group from chromatin compacts the complex and stops gene

expression. Histone deacetylase (HDAC) is an enzyme that removes the acetyl group to restore the positive charges on the lysine residues and thus suppresses gene transcription, potentially causing cancer since inappropriate silencing of tumor suppressor genes can lead to tumor formation. Therefore, inhibitors of HDAC play an important role in stopping the progression of cancer by expressing the silenced gene¹.

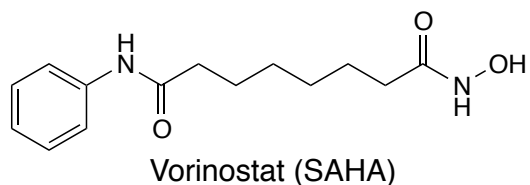
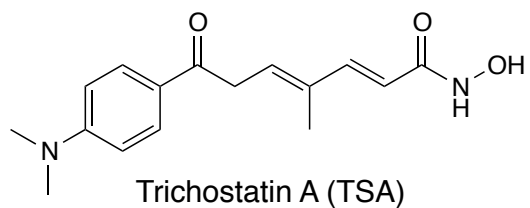
The mechanism of antitumor activity of HDAC inhibitors is not entirely clear. Theories include dysregulation of genes involved in cell cycle progression, differentiation, and apoptosis. HDAC inhibitors appear to be effective against hematological and epithelial tumor sources by having a role in cell cycle arrest, apoptosis, antiangiogenesis. The effect that occurs from HDAC inhibitor treatment appears to be dependent on the tumor cell rather than the specific HDAC inhibitors used¹.

HDAC inhibitors are currently being explored in the treatment of stomach, colorectal, and renal cancers. Annually, there are about 217,000 new cases and 82,000 deaths that result from these cancers^{2,3}. Surgical treatment is the main mode of therapy for treating these types of cancer making it important to find a pharmacologic option that can improve the quality of life of patients and decrease healthcare costs⁴.

HDACs are a family of enzymes that consist of four major classes that differ in their structure and function. Classes I, II, and IV are metalloenzymes that contain a zinc component of the active site and are targeted by the HDAC inhibitors currently in development for anti-cancer activity¹. Class III HDACs are considered sirtuins and are all NAD⁺-dependent proteases⁵. They are not inhibited by classical (class I, II, IV) inhibitors but are inhibited by nicotinamide, also known as vitamin B3¹. Among the classes of HDACs, there are 18 different isozymes, 11 of which are metalloenzymes⁶.

Inhibitors of HDAC classes I, II, and IV can be differentiated into four main groups of compounds: small molecule hydroxamates, cyclic tetrapeptides, benzamides, and short-chain fatty acids⁵. These four classes can be generalized by having a common pharmacophore, which is essential for the interaction with the enzyme. This pharmacophore incorporates a hydrophobic cap that hinders access to the active site, a polar site, and a hydroxamic acid type zinc-binding site¹. The zinc-binding site is separated by a hydrophobic spacer with optimal length that spans the hydrophobic pocket of the enzyme¹.

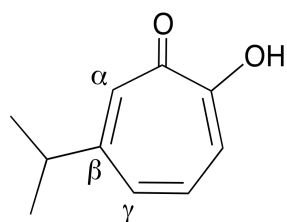
Hydroxamic acids are the largest class of HDAC inhibitors. Compounds containing hydroxamic acid residues bind to the HDAC catalytic site with high affinity, blocking access of the substrate to the zinc ion. Compounds of this class are very potent but are reversible inhibitors of HDAC classes I, II, and IV. Trichostatin A (TSA) was one of the first hydroxamic acids developed but was found to be toxic and lack specificity. This led to the development of suberoylanilide hydroxamic acid (SAHA), also known as vorinostat, a second-generation compound currently approved for the treatment of cutaneous T-cell lymphoma that causes cell growth arrest, differentiation, and/or apoptosis. Hydroxamic acids, as well as benzamides, are the focus of development for new compounds as these compounds have a better HDAC inhibitory profile and lower toxicity risk compared to other classes of HDAC inhibitors¹.



Importance of Current Project

The inhibitor compounds of class I, II, and IV in development have exhibited toxicity, creating the need of developing HDAC inhibitor compounds specific to certain HDAC enzymes in order to decrease the prevalence of toxicity. Current HDAC inhibitor compounds in clinical trials are considered to be active against a range of HDAC isozymes and have demonstrated toxicity, likely related to the inhibition of the many functions of HDAC isozymes. Ideally inhibitors should be designed for activity against specific HDAC isozymes in order to improve efficacy and reduce toxicity. Class I isozymes, which include HDAC 1, 2, 3, and 8, tend to be over-expressed in certain tumors, such as HDAC 2 in colon cancer, and correlate with poor prognosis. Class II, which include HDAC 4, 5, 6, 7, 9, and 10 have been correlated with better prognosis. Mice knockout experiments of HDAC 3, 5, and 9 show adverse cardiac toxicity indicating that inhibitors that target these isozymes may cause toxicity. Thus, it appears that designing a class I inhibitor compound, especially one with activity against HDAC 1, 2 or 8, would be an attractive strategy⁶.

β -thujaplicin, is a natural product isolated from the heartwood of trees in the cupressaceae family in the early 1950s. It has been shown to have activity against melanoma and prostate cancer cell lines and a related compound, α -thujaplicin, has demonstrated activity



β -Thujaplicin

against lymphocytic leukemia and stomach cancer lines. β -thujaplicin is characterized by a low molecular weight and allows for structural modification⁶.

Derived from β -thujaplicin is the tropolone scaffold, which is a unique structure that allows for both potency and selectivity. The scaffold allows for a zinc metal binding portion (the α -hydroxy ketone), a lipophilic seven-

membered ring that interacts with the hydrophobic pocket surrounding the zinc ion via three possible positions: α , β , γ . These unique positions allow for substitution to reach important pockets in the HDAC isozyme⁶.

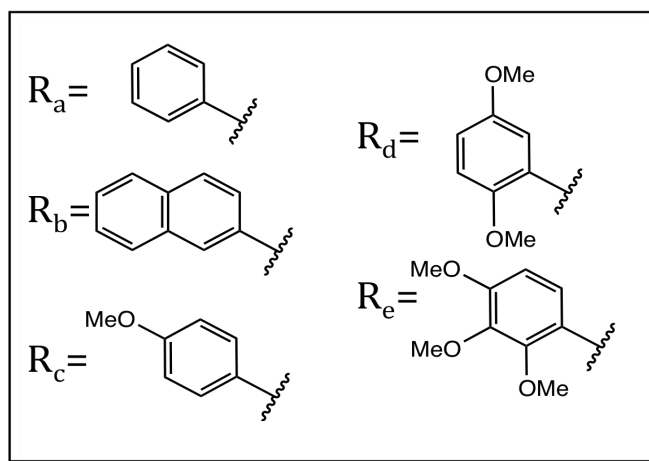
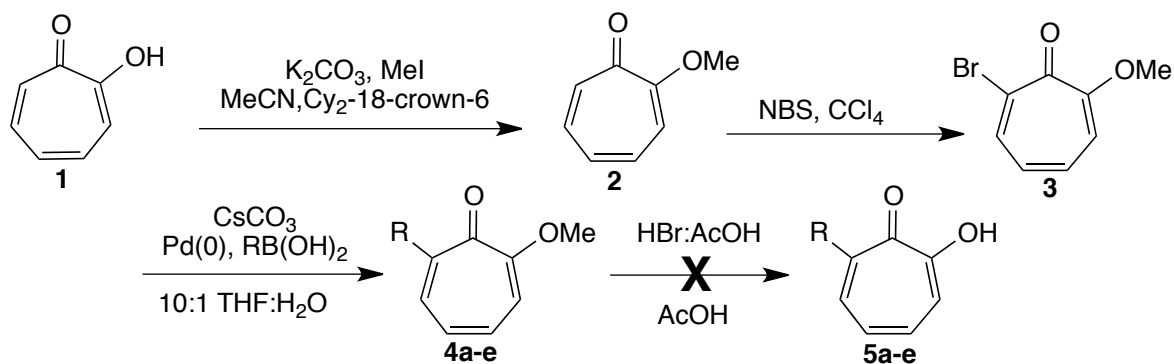
Compared to hydroxamates, an alternative class of HDAC inhibitors based on the tropolone scaffold may yield several advantages. While both classes include a metal-targeting moiety, the tropolone class possesses important distinctions in terms of metabolic stability and isozyme selectivity. Hydroxamates, such as vorinostat, have relatively short metabolic half-lives as a result of an easily reduced N-O bond, a hydrolytically labile amide linkage and the formation of glucuronides. In comparison, the metal-targeting moiety of the tropolone class would not be at risk of reductive or hydrolytic transformations due to its vinylogous carboxylic acid. Another unique advantage for the tropolone is that its scaffold offers multiple points of variation and access to pockets in proximity to the metal binding site that may impart isozyme selectivity, thereby reducing toxicity and increasing efficacy⁶.

Results and Discussion:

As β -substituted compounds have previously been reported by our research group⁷, the goal of this project is to optimize the α -position of the tropolone scaffold by placing groups with diverse functionality through late stage analog synthesis. Thus we needed to develop an efficient synthetic route that would allow for development of numerous analogs.

We initially developed a 5-step synthesis (**scheme 1**) to obtain our tropolone analogs. Our synthesis began with the esterification of commercially available tropolone **1** with iodomethane by following the procedure reported by Koodanjeri, et al⁸ to produce methyl protected tropolone **2**.

Scheme 1.



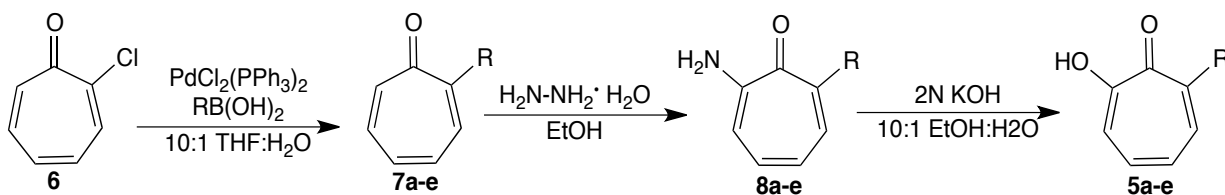
The purpose was to add an easily removable hydroxyl protecting group on the tropolone in order to be able to add desired substituents in the α -position. The next step was to add a halogen on the tropolone ring in order to run Suzuki cross-coupling reactions. Bromine was the halogen of choice due to its increased reactivity towards palladium insertion and this was achieved by use of N-bromosuccinamide and carbon tetrachloride. We witnessed excess bromination at this step, and careful purification with silica gel column chromatography was required to obtain **3**. The last step of de-protecting the methyl group proved to be difficult as our

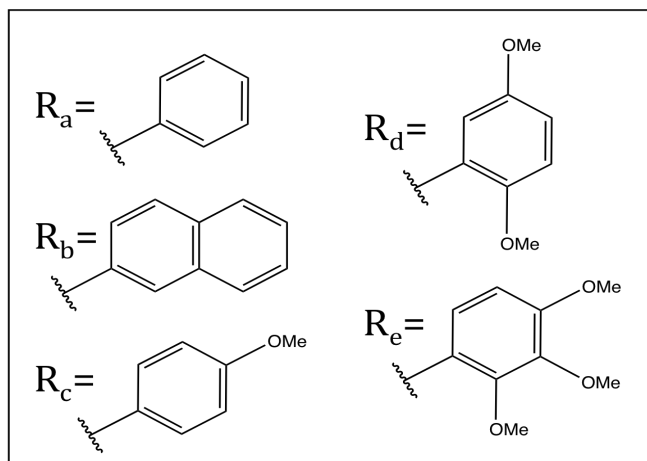
conditions of HBr and acetic acid were not able to yield the final product. Conditions of BBr₃ and CH₂Cl₂ did not work as well.

Since the problem was in the de-protecting step, we decided to try adding other protecting groups besides methyl, such as methoxymethyl, that would allow for Suzuki coupling reactions but would also be easy to remove for the hydrolysis to the final product. However, these other attempts proved to be unsuccessful at obtaining the intermediary products as the less stable protecting groups rapidly decomposed and thus we were unable to proceed to the Suzuki coupling reactions.

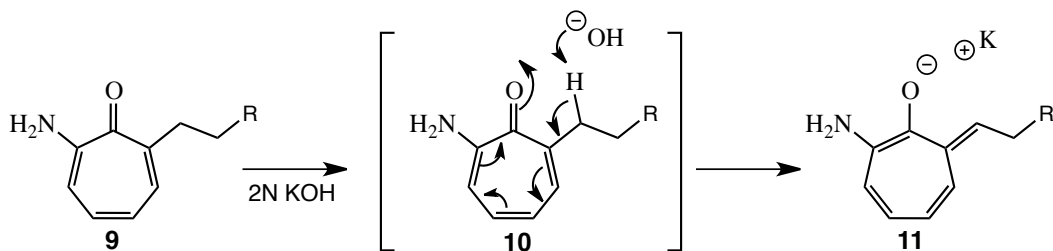
After these attempts, we developed an alternative route as seen in **scheme 2** to obtain our tropolone derivatives based on a protocol previously reported for the synthesis of α -thujaplicin⁹. Starting from a commercially available chlorotropone **6**, we were able to immediately run Suzuki cross-coupling reactions in order to prepare a series of lipophilic compounds with substitutions at the α -position **7a-e** and thus this route cut a step from our original synthesis in **scheme 1**. After coupling the desired groups, the addition of hydrazine led to the corresponding 7-aryl 2-amino tropones **8a-e**. Final hydrolysis of the amino-tropones under basic conditions yielded the α -substituted tropolones **5a-e** in good overall yield.

Scheme 2.

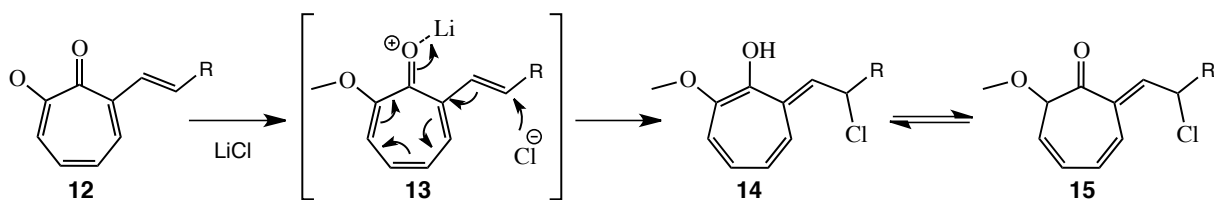




We then aimed to add substituents that would have extended lipophilic chains. Since our synthetic route in **scheme 2** was effective, we used it to add our desired groups on, with slight modification. As our desired groups were aliphatic chains, we ran our palladium couplings utilizing grignard reagents in Kumada cross-coupling conditions. The coupling and subsequent hydrazine reactions achieved our desired derivatives but the hydrolysis step did not yield our final product. Upon NMR analysis of the final product, it appeared that our product did not hydrolyze in place of the hydrazine and it is theorized that it instead pulled an allylic proton on the aliphatic linker **10**. The proposed mechanism can be seen below (**9-11**), whereas the potassium trapped enolate extinguished the system's reactivity. Realizing this problem would apply to our other aliphatic linker compounds, we tried our synthesis using the bromo-methoxy material in **scheme 1** to avoid this problem in the hydrolysis step. Unfortunately, due to the basicity of the grignard reagents, the kumada coupling conditions yielded a Favorskii rearrangement. Thus, we were forced to change our conditions and we decided to try to use Suzuki couplings with boronic acids.

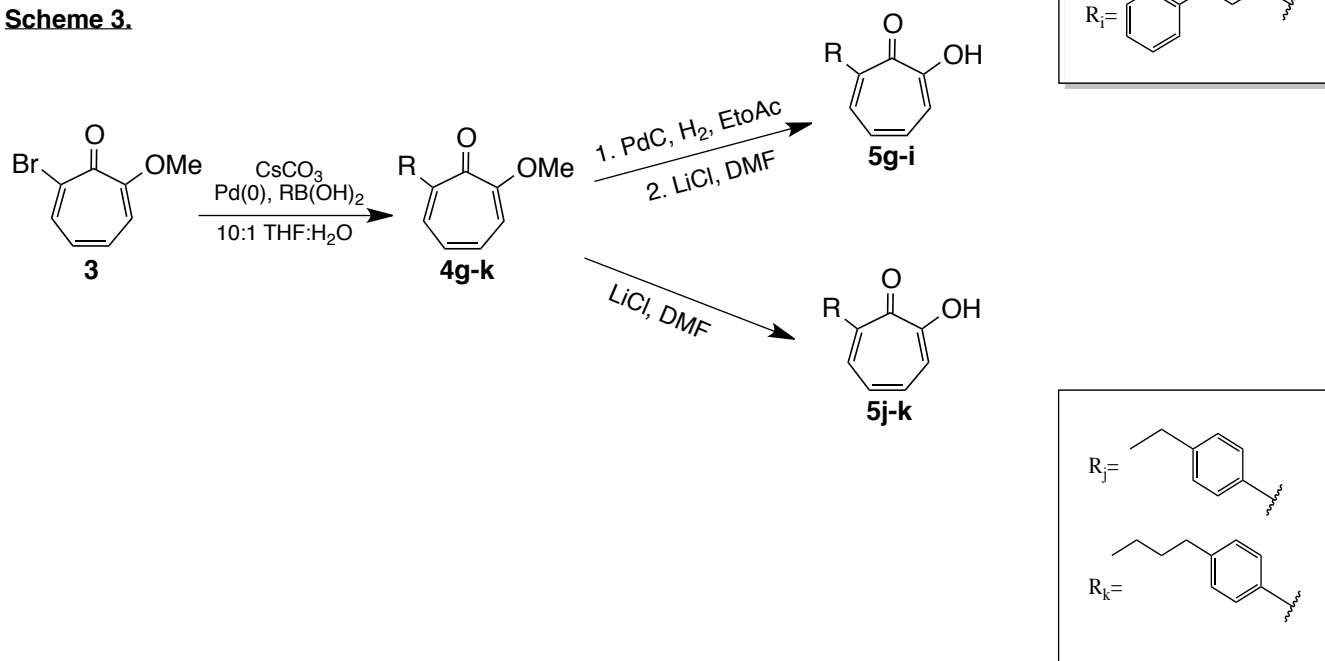


But to continue with the original **scheme 1**, we determined we needed an alternative de-protection method in order to obtain the final analog. We tried various basic conditions such as KOH, H₂SO₄, Na₂O₂, and LiOH, all leading to failed attempts. Eventually we found in the literature the LiCl in DMF conditions. However, we noticed that LiCl worked except for groups that had an alkene in the aliphatic linker as the chlorine would insert in the alkene of the aliphatic chain. The proposed mechanism can be seen in **12-15**.



To overcome this we decided to buy terminal boronic acids and then hydrogenate the intermediates after the coupling to avoid the chance of LiCl insertion. The nucleophilic de-protection scheme with of LiCl then worked to de-protect the methyl group and we were able to develop five more compounds (**scheme 3**).

Scheme 3.



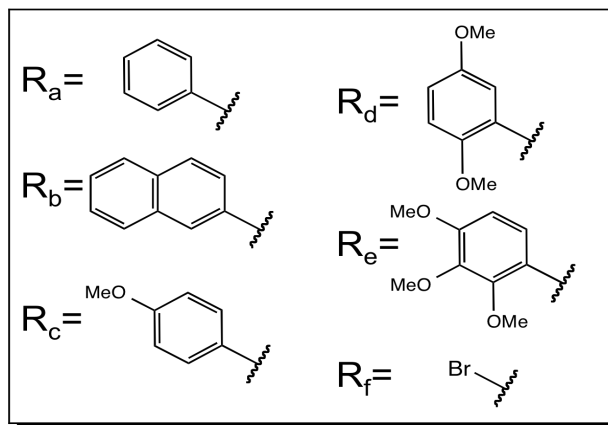
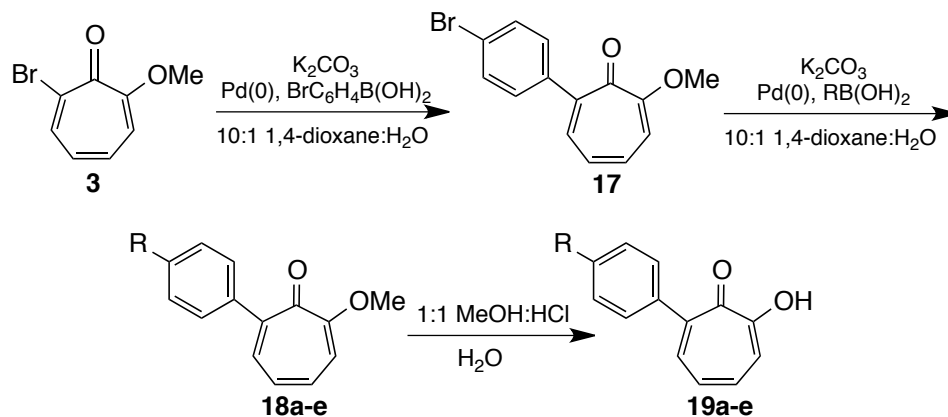
Our next efforts were focused on producing compounds that had extended aromatic chains. When looking for more commercially available boronic acids, we found 4-Bromophenylboronic acid. We recognized this as a potential tropolone derivative and as well as a building block, since we could couple to the boronic acid and then run another Suzuki coupling to substitute the bromine with another group. We decided to use the synthesis route seen in **scheme 1** for this group of analogs as it was more efficient. The bromo-methoxy route would allow for a large-scale build up of intermediates and allow for late stage synthetic elaboration to construct the desired analogs.

Using our now modified route with an improved LiCl de-protection step, we were able to obtain the desired final compounds but we discovered a few issues. The first was that upon NMR analysis, the proton peaks showed the compound with some impurity in the aromatic region. Liquid chromatography mass spectroscopy (LCMS) showed that along with our product, we had multiple homo-coupled para-bromo impurities **16**. We theorize this to be due to excess boronic acid being able to couple to the bromide on the newly coupled para-bromo tropone. To overcome this issue, we initially decreased the equivalents of the boronic acid to 1.5 and then eventually to 0.9. We found that the 1.5 equivalents had less of the poly-coupled para-bromo compound compared to the 2 equivalents but that 0.9 equivalents had minimal of this impurity with a relatively smaller yield. Thus, we thus changed our reaction conditions to 0.9.

The next problem was the significant grease peaks in the 0-1 range in the proton NMR. This was consistent with all compounds we made and only at the final step of the synthesis. We theorized that either the reaction conditions caused some decomposition of the compound since we ran the reaction at 160°C or there were some impurities in the LiCl or the DMF. We changed our LiCl, DMF, and glass vials in which reactions ran, but still found grease in the NMR analysis.

Thinking that the de-protection reaction of LiCl had some role in the grease issue, we then switched to another de-protection method from the literature using methanol/H₂O. Since we found that this method was free of grease and since this method involves recrystallization instead of purifying the compound with silica gel column chromatography, we hypothesize that the grease was due to our compound stripping some binders from the silica gel column chromatography. Having overcome these problems, we were able to produce more analogs as seen in **scheme 4**.

Scheme 4.

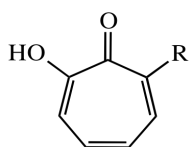


Biological Data:

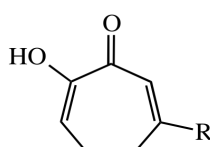
In order to learn more about the structure activity relationship of our compounds and tailor future work to develop compounds with isozyme specificity and potent biological activity, we tested our compounds against various HDAC isozyme lines (**table 1**) and various cell lines (**table 2**).

Table 1. Inhibition of HDAC Isozymes

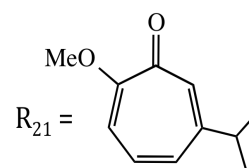
Compound	HDAC Isozyme (Ki values in nM)					
	1	2	8	4	5	6
TSA	0.87	1.06	69.65	14,547	4,120	3.02
5a	NA	0.26	1.09	NA	NA	527
5b	NA	0.25	186.30	NA	NA	NA
5c	NA	0.81	83.80	NA	NA	NA
5d	NA	0.42	811.50	NA	NA	NA
5e	NA	0.23	123.65	NA	NA	NA
20a	NA	0.06	1.47	10,860	NA	NA
20b	NA	0.12	2.38	8,361	NA	NA
20c	NA	0.51	266.30	11,204	NA	NA
20d	NA	0.13	12.81	806.13	NA	NA
20e	NA	0.22	2.27	6115	NA	NA
20f	NA	0.04	122.70	990.23	NA	NA
β -thujiplicin	NA	15.44	177.95	NA	NA	NA
21	NA	NA	7.87	11,641	NA	NA



R_{5a} = phenyl
 R_{5b} = 2-naphthyl
 R_{5c} = 4-OMe-phenyl
 R_{5d} = 2,5-OMe-phenyl
 R_{5e} = 2,3,4-OMe-phenyl



R_{20a} = phenyl
 R_{20b} = 4-OMe-phenyl
 R_{20c} = 2,5-OMe-phenyl
 R_{20d} = *t*-butyl
 R_{20e} = *sec*-butyl
 R_{20f} = cyclopentyl



We tested our first five analogs developed at the α -position as well as some of the previously reported β -substituted compounds (**20a-f**, **21**)⁷ to compare their biologic activity

against the various HDAC isozymes. We tested these compounds by use of Michaelis-Menten analysis of six different HDAC isozymes: 1, 2, 4, 5, 6, and 8⁶. These results show that a few analogs have very good biological activity in two different HDAC isozymes (2 and 8) from HDAC class I and that both our α - and β -substituted tropolones function as potent inhibitors of HDAC 2. As seen in **table 1**, seven of our compounds demonstrate high levels of selectivity (greater than 100-fold) for the inhibition of HDAC isozyme 2 compared to HDACs 1, 4, 5, 6, and 8. Besides β -thujaplicin, all hydrolyzed compounds were more potent inhibitors of HDAC2 than TSA, which exhibits pan-HDAC inhibition. Compared to free tropolones, methylated tropolone **21** shows significantly lower activity, indicating that the ionizable α -hydroxy ketone may facilitate strong zinc chelation of the HDAC active site.

Interestingly, some of the compounds (**5a**, **20a**, **20b**, and **20e**) included HDAC 8 inhibition at lower K_i values than those of both TSA and vorinostat at 69.95 and 480 nM, respectively. The results also indicate that increasing steric bulk at the α -position was associated with loss of potency whereas increasing steric bulk at the β -position showed variable effects against HDAC 8.

Knowing that our compounds had excellent activity against HDAC2, we wanted to see if this translated to cellular effects (**table 2**), thus judging their potential as drug candidates. Since it has been established that HDAC inhibitors have anti-proliferative effects against hematological cancer cell lines, we tested our compounds against two T-cell lymphocyte lines: HuT078 and Jurkat⁶. We also chose a colon cancer cell line, HCT116, and a pancreatic cancer cell line, BxPC-3) to test activity in solid tumor lines.

Table 2. Inhibition of Cell Growth

Compound	Cell Line (GI ₅₀ values in mM)				
	Jurkat	HuT-78	HCT-116	BxPC-3	hDF
5a	3.33	7.83	15.24	29.39	96.46
5b	1.15	4.11	32.06	17.1	93.07
5c	0.62	2.87	56.99	35.93	>100
5d	0.76	3.05	46.65	14.1	>100
5e	1.86	4.74	34.98	21	>100
20a	0.67	4.14	53.44	18.5	>100
20b	4.62	8.95	43.67	91.6	>100
20c	5.89	17.09	>100	34.79	>100
20d	4.45	13.11	62.61	43.02	>100
20e	0.59	3.25	26.86	104	>100
20f	6.30	11.36	>100	180	>100
β -thujaplicin	1.10	4.99	6.92	19	>100
21	>100	>100	>100	>100	>100
Vorinostat	0.90	2.10	2.50	5.56	18.95

Tropolone analogs **5c**, **5d**, **20a** and **20e** showed significant half maximal growth inhibition (GI₅₀) in both hematological T-lymphocyte cell lines. Additionally, these compounds showed increased activity relative to vorinostat against the Jurkat cell line, having GI₅₀ values less than 1 mM. In the HCT-116 line, tropolones were less active but two derivatives, **5a** and β -thujaplicin, showed GI₅₀ values less than 20 μ M. Similarly, in the BxPC-3 cells, **5b**, **5d**, **20a** and β -thujaplicin had GI₅₀ values less than 20 μ M.

We also tested our compounds against a non-malignant human dermal fibroblast line to assess toxicity of our compounds on normal cells. The results indicated a lack of general cytotoxicity with our compounds, with most derivatives showing no activity at 100 μ M. This

value is significantly greater compared to vorinostat, indicating that our tropolones require higher concentrations in order to notice cytotoxic effects.

Recently, our compounds have been screened in mouse-derived organoids to assess its ability as preventative colon cancer agents. These organoids are multicellular crypt-like structures that are derived from adult intestinal stem cells, embryonic stem cells, or induced pluripotent stem cells and can function as a tissue surrogate. The organoid included cells that possessed Math1 is a transcription factor that regulates secretory cell differentiation as well as a more mature differentiation marker, Muc2. Compounds that enhance differentiation and increase Math1 expression may have chemo-preventative properties. It is believed that reduced expression of Math1 may result in cancer development due to suppression of growth-regulating differentiation pathway or by allowing the tissue more susceptible to inflammation from reduced production of mucus. Broad-spectrum HDAC inhibitors, TSA and vorinostat, were found to increase commitment to the secretory cell lineage by increasing both Math1 and Muc2. Our compounds increased Math1 with minimal Muc2 effect, which the authors' attributed to the selectivity of our compounds¹⁰.

Conclusion

This project describes our efforts to develop selective and potent histone deacetylase inhibitors at the based on the unique tropolone scaffold as potential anti-cancer drug candidates. Our work focused on the α -position in order to optimize the structure activity relationship for that position. We tested the biologic activity for some of our compounds and they appear to be selective and have good activity against HDAC isozymes 2 and 8.

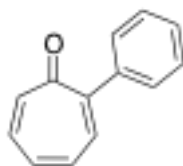
Currently our project still remains ongoing as we continue to produce α -substituted compounds and learn more about the ideal structure activity relationship of these HDAC compounds. Ideally, our second and third set of compounds will be tested for biological activity in order to compare to our first set of compounds to further outline the direction of the project. Some ongoing works to increase our library of analogs include making aniline, heterocycles, and sulfonamide analogs. We also started some initial work on γ -substituted compounds but more focus is needed to find an efficient synthetic route to develop these analogs. Our group intends to have multi-substituted analogs to increase specificity to and activity against various HDAC isozymes.

References

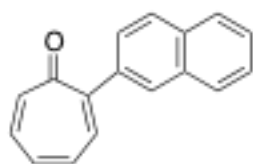
1. Acharya MR, Sparreboom A, Venitz J, Figg WD. Rational development of histone deacetylase inhibitors as anticancer agents: a review. *Mol Pharmacol*. 2005; 68(4): 917-932.
2. Catalano V, Labianca R, Beretta GD, Gatta G, de Braud F, Van Cutsem E. Gastric cancer. *Crit Rev Onc Hemat*. 2009; 71(2):127-164.
3. Gatta G, Ciccolallo L, Capocaccia R, Coleman M, Hakulinen T, Moller H, Berrino F. Differences in colorectal cancer survival between European and US populations: the importance of sub-site and morphology. *Eur J Cancer*. 2003; 39:2214-2222.
4. Segal NH, Saltz, LB. Evolving Treatment of Advanced Colon Cancer. *Annu Rev Med*. 2009; 60(1):207-219.
5. Valente S, Mai A. Small-molecule inhibitors of Histone Deacetylase for the treatment of cancer and non-cancer diseases: a patent review (2011-2013). *Expert Opin Ther Pat*. 2014; 24(4):401-415.
6. Ononye SN, VanHeyst MD, Oblak EZ, et al. Tropolones as leadlike natural products: The development of potent and selective histone deacetylase inhibitors. *ACS Med Chem Lett*. 2013;4:757-761.
7. Oblak, EZ, Bolstad E, Priestley N, Hadden MK, Wright D. The furan route to tropolones: probing the antiproliferative effects of β -thujaplicin analogs. *Org Biomol Chem*. 2012; 10:8597-8604.
8. Koodanjeri S, Joy A, Ramamurthy V. Asymmetric induction with cyclodextrins: photocyclization of tropolone alkyl ethers. *Tetrahedron*. 2000; 56:7003-7009.
9. Noyori R, Makino S, Okita T, Hakyakawa Y. A method for the generation of a synthetic equivalent of unsubstituted oxyallyl via the bromo ketone-iron carbonyl reaction: a new route to thujaplicins. *J Org Chem*. 1975; 40:806-807.
10. Cao L, Kuratnik A, Xu W, Gibson JD, Kolling F 4th, Falcone ER, Ammar M, Van Heyst MD, Wright DL, Nelson CE, Giardina C. Development of intestinal organoids as tissue surrogates: Cell composition and the epigenetic control of differentiation. *Mol Carcinog*. 2013; 1-14.

Experimentals:

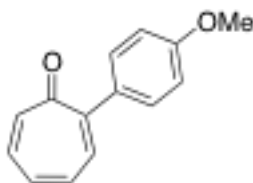
General Procedure For Suzuki Couplings: 2-Chloro-2,4,6-cycloheptatrien-1-one (1.0 eq), aryl boronic acid (2.0 eq), and cesium carbonate (4.0 eq) were added to 10:1 THF/H₂O (0.2 M) and the mixture was thoroughly degassed by bubbling argon through solution (10 min). Bis(triphenylphosphine)palladium(II) dichloride (0.1 eq) was added and the mixture was again degassed with argon (5 min). The homogenous solution was heated at 75 °C for 16 h before being cooled to room temperature. Water was added and the mixture was extracted with EtOAc (3 x). The combined organic layers were washed with brine, dried over Na₂SO₄, filtered and concentrated *in vacuo*. Flash chromatography of the crude residue (SiO₂, EtOAc in hexanes) provided the desired 2-aryl-tropones.



2-phenyl tropone 2a: 99 % yield; R_f = 0.5 (1:1 EtOAc:Hexanes); M_p = 77.9-79.2 °C; IR (KBr): ν: 3101, 3022, 1895, 1808, 1625, 1547, 1441, 1261, 784, 698. ¹H NMR (500 MHz, CDCl₃) δ 7.51-7.49 (m, 2H), 7.43-7.36 (m, 4H), 7.20 (d, J = 12.2 Hz, 1H), 7.14 (ddd, J = 19.8, 1.3, 1.3, 1.3, 1.4 Hz, 1H), 7.07-7.03 (m, 1H), 6.99-6.95 (m, 1H). ¹³C NMR (126 MHz, CDCl₃) δ 186.4, 152.4, 142.2, 139.9, 136.5, 135.2, 133.7, 133.2, 129.0, 128.3, 128.0. HRMS (ESI) calcd for C₁₃H₁₁O [M+H]⁺: 183.0810; found: 183.0788.

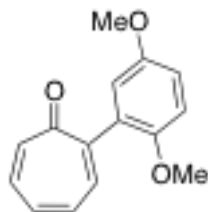


2-naphthyl tropone 2b: 98 % yield isolated with inseparable impurity that is removed during amination; R_f = 0.58 (1:1 EtOAc:Hexanes); M_p = N/A; IR (KBr): ν: 3056, 3009, 2359, 1926, 1876, 1771, 1703, 1626, 1574, 800, 777, 733, 697. ¹H NMR (500 MHz, CDCl₃) δ 7.92 (d, J = 1.45 Hz, 1H), 7.90 (d, J = 2.0 Hz, 1H), 7.71 (d, J = 8.3 Hz, 1H), 7.57-7.45 (m, 3H), 7.41 (dd, J = 6.9, 0.85, 0.90 Hz, 1H), 7.38-7.36 (m, 1H), 7.26 (d, J = 12.1 Hz, 1H), 7.20-7.16 (m, 1H), 6.99-6.97 (m, 2H). ¹³C NMR (126 MHz, CDCl₃) δ 186.4, 152.6, 141.7, 138.3, 137.6, 135.5, 133.8, 133.5, 133.2, 130.7, 128.3, 128.2, 126.4, 125.9, 125.6, 125.2, 125.2. HRMS (ESI) calcd for C₁₇H₁₃O [M+H]⁺: 233.0966; found: 233.0945.

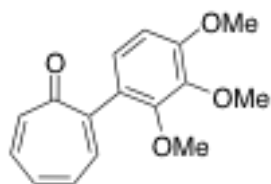


2-(4-methoxy-phenyl) tropone 2c: 99 % yield; R_f = 0.59, (1:1 EtOAc:Hexanes); M_p = 52.2-53.6 °C; IR (KBr): ν: 2958, 2835, 2541, 2041, 1974, 1883, 1622, 1564, 1175, 1031, 830, 780, 686. ¹H NMR (500 MHz, CDCl₃) δ 7.51 (d, J = 2.0 Hz, 1H), 7.50 (d, J = 2.0 Hz, 1H), 7.40 (d, J = 9.0 Hz, 1H), 7.23 (d, J = 12.1 Hz, 1H), 7.15 (ddd, J = 21.5, 1.2, 1.2, 1.2, 1.2 Hz, 1H), 7.06 (t, J = 20.0, 10.1, 9.5 Hz, 1H), 6.99-6.94

(m, 3H), 3.85 (s, 3H). ^{13}C NMR (126 MHz, CDCl_3) δ 186.5, 159.9, 152.0, 142.0, 136.0, 135.3, 133.8, 132.8, 132.1, 130.6, 113.6, 55.3. HRMS (ESI) calcd for $\text{C}_{14}\text{H}_{13}\text{O}_2$ $[\text{M}+\text{H}]^+$: 213.0916; found: 213.0898.

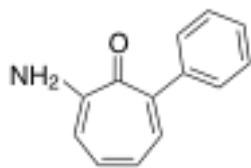


2-(2,5-methoxy-phenyl) tropone 2d: 96 % yield; R_f = 0.29 (1:1 EtOAc:Hexanes); M_p = 102.2-103.2 $^\circ\text{C}$; IR (KBr): ν : 2940, 2832, 2351, 1628, 1588, 1218, 1046, 808, 748, 694. ^1H NMR (500 MHz, CDCl_3) δ 7.30 (dd, J = 8.4, 1.0, 1.1 Hz, 1H), 7.15-7.13 (m, 2H), 7.03-6.94 (m, 2H), 6.88 (s, 1H), 6.88 (s, 1H), 6.82 (t, J = 3.2, 1.6, 1.6 Hz, 1H), 3.79 (s, 3H), 3.74 (s, 3H). ^{13}C NMR (126 MHz, CDCl_3) δ 186.5, 153.7, 150.9, 150.3, 141.0, 136.3, 134.9, 133.5, 133.3, 130.9, 116.4, 114.1, 112.5, 56.5, 55.7. HRMS (ESI) calcd for $\text{C}_{15}\text{H}_{15}\text{O}_3$ $[\text{M}+\text{H}]^+$: 243.1021; found: 243.1016.

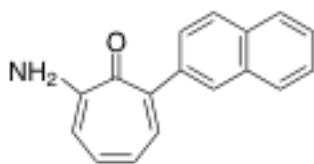


2-(2,3,4-methoxy-phenyl) tropone 2e: 91 % yield; R_f = 0.29 (1:1 EtOAc:Hexanes); M_p = 98.3-99.6 $^\circ\text{C}$; IR (KBr): ν : 2946, 2841, 2825, 1947, 1883, 1626, 1583, 1458, 1103, 1072, 1013, 799, 684. ^1H NMR (500 MHz, CDCl_3) δ 7.28 (dd, J = 9.6, 1.1, 1.1 Hz, 1H), 7.18-7.12 (m, 2H), 7.03-6.93 (m, 3H), 6.72 (d, J = 8.5 Hz, 1H), 3.89 (s, 3H), 3.88 (s, 3H), 3.82 (s, 3H). ^{13}C NMR (126 MHz, CDCl_3) δ 187.0, 154.2, 150.7, 150.6, 141.9, 140.6, 136.3, 135.1, 133.6, 133.1, 127.7, 124.6, 107.3, 60.9, 60.7, 56.0. HRMS (ESI) calcd for $\text{C}_{16}\text{H}_{17}\text{O}_4$ $[\text{M}+\text{H}]^+$: 273.1127; found: 273.1118.

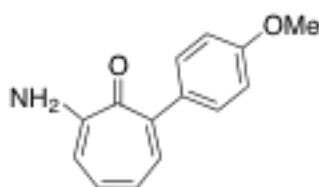
General Procedure For α -Amination of 2-aryl tropone: To a solution of α -aryl-tropone (1.0 eq) in EtOH (0.2 M) was added 65 % hydrazine monohydrate (25 eq). The solution was allowed to stir at room temperature until all starting material was consumed by monitoring on TLC (~45 min). The reaction was concentrated *in vacuo* and then taken up in EtOAc (0.05 M) and washed with H_2O (3 x). The organic layer was then washed with brine, dried over Na_2SO_4 , filtered and concentrated *in vacuo*. Flash chromatography of the crude residue (SiO_2 , EtOAc in hexanes) provided the desired α -amino-tropones.



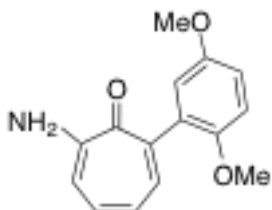
7-amino-2-phenyl tropone 3a: 88 % yield; R_f = 0.61 (4:1 EtOAc:Hexanes); M_p = 209.3-210.4 $^\circ\text{C}$; IR (KBr): ν : 3403, 3251, 3122, 1604, 1515, 1428, 1336, 1235, 1054, 919, 686. ^1H NMR (500 MHz, CD_2Cl_2) δ 7.50-7.38 (m, 5H), 7.33 (t, J = 14.4, 7.1, 7.3 Hz, 1H), 7.14 (t, J = 20.2, 10.1, 10.1 Hz, 1H), 6.93 (d, J = 10.0 Hz, 1H), 6.77 (t, J = 19.6, 9.8, 9.8 Hz, 1H), 6.12 (s, 2H). ^{13}C NMR (126 MHz, CD_2Cl_2) δ 174.9, 158.5, 143.4, 142.5, 139.0, 135.8, 130.1, 128.3, 127.7, 123.4, 112.7. HRMS (ESI) calcd for $\text{C}_{13}\text{H}_{12}\text{NO}$ $[\text{M}+\text{H}]^+$: 198.0919; found: 198.0900.



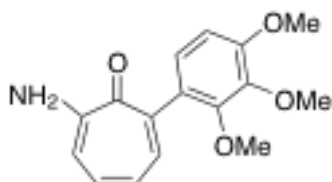
7-amino-2-naphthyl tropone 3b: 89 % yield; R_f = 0.63 (4:1 EtOAc:Hexanes); M_p = 221.7-222.5 °C; IR (KBr): ν : 3443, 3280, 3150, 1604, 1511, 1446, 1062, 780, 737. ^1H NMR (500 MHz, CD_2Cl_2) δ 7.90 (d, J = 8.2 Hz, 1H), 7.87 (d, J = 8.3 Hz, 1H), 7.55-7.45 (m, 4H), 7.38-7.35 (m, 2H), 7.23 (td, J = 20.2, 10.1, 10.1, 1.1, 1.1, 1.1 Hz, 1H), 6.98 (d, J = 9.9 Hz, 1H), 6.80 (t, J = 19, 9.5, 9.5 Hz, 1H), 6.13 (s, 2H). ^{13}C NMR (126 MHz, CD_2Cl_2) δ 175.2, 157.9, 141.8, 141.8, 139.6, 136.5, 134.0, 132.2, 128.8, 128.1, 126.9, 126.4, 126.3, 126.2, 126.1, 123.2, 112.8. HRMS (ESI) calcd for $\text{C}_{17}\text{H}_{14}\text{NO}$ $[\text{M}+\text{H}]^+$: 248.1075; found: 248.1065.



7-amino-2-(4-methoxy-phenyl) tropone 3c: 87 % yield; R_f = 0.55 (4:1 EtOAc:Hexanes); M_p = 153.8-155.2 °C; IR (KBr): ν : 3434, 3269, 3233, 2962, 1601, 1511, 1450, 1244, 1023, 829, 781. ^1H NMR (500 MHz, CD_2Cl_2) δ 7.49 (dd, J = 9.6, 1.0, 0.9 Hz, 1H), 7.44-7.41 (m, 2H), 7.10 (td, J = 20.0, 1.0, 1.0, 1.0 Hz, 1H), 6.96-6.93 (m, 2H), 6.89 (d, J = 10.0 Hz, 1H), 6.24 (s, 2H), 3.83 (s, 3H). ^{13}C NMR (126 MHz, CD_2Cl_2) δ 174.9, 159.5, 158.4, 141.9, 138.7, 135.6, 135.4, 131.3, 123.3, 113.7, 112.9, 55.8. HRMS (ESI) calcd for $\text{C}_{14}\text{H}_{14}\text{NO}_2$ $[\text{M}+\text{H}]^+$: 228.1025; found: 228.1018.

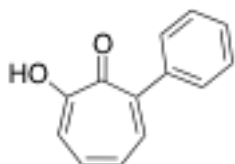


S13 7-amino-2-(2,5-methoxy-phenyl) tropone 3d: 84 % yield; R_f = 0.39 (4:1 EtOAc:Hexanes); M_p = 109.6-110.7 °C; IR (KBr): ν : 3278, 3191, 2939, 2831, 1601, 1519, 1455, 1219, 1047, 783, 725. ^1H NMR (500 MHz, CD_2Cl_2) δ 7.39 (d, J = 9.5 Hz, 1H), 7.12 (t, J = 20.2, 10.1, 10.1 Hz, 1H), 6.92-6.87 (m, 3H), 6.80 (d, J = 2.9 Hz, 1H), 6.72 (t, J = 19.5, 9.7, 9.8 Hz, 1H), 6.42 (s, 2H), 3.77 (s, 3H), 3.69 (s, 3H). ^{13}C NMR (126 MHz, CD_2Cl_2) δ 174.5, 158.1, 154.1, 151.5, 139.8, 138.9, 136.2, 133.9, 122.6, 117.1, 113.4, 112.9, 112.6, 56.7, 56.2. HRMS (ESI) calcd for $\text{C}_{15}\text{H}_{16}\text{NO}_3$ $[\text{M}+\text{H}]^+$: 258.1130; found: 258.1151.

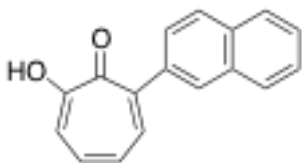


7-amino-2-(2,3,4-methoxy-phenyl) tropone 3e: 86 % yield; R_f = 0.42 (4:1 EtOAc:Hexanes); M_p = 175.3-176.5 °C; IR (KBr): ν : 3367, 2939, 2825, 1599, 1514, 1455, 1097, 1019, 770. ^1H NMR (500 MHz, CDCl_3) δ 7.41 (d, J = 9.5 Hz, 1H), 7.09 (t, J = 20.1, 10.0, 10.1 Hz, 1H), 6.91 (d, J = 8.5 Hz, 1H), 6.87 (d, J = 10 Hz, 1H), 6.72-6.68 (m, 2H), 6.28 (s, 2H), 3.99 (s, 3H), 3.87 (s, 3H), 3.73 (s, 3H). ^{13}C NMR (126 MHz, CDCl_3) δ 174.4, 157.2, 153.1, 151.3, 142.0, 139.3, 138.7, 135.4, 129.7, 124.5, 122.4, 112.4, 107.4, 60.9, 60.7, 55.9. HRMS (ESI) calcd for $\text{C}_{16}\text{H}_{18}\text{NO}_4$ $[\text{M}+\text{H}]^+$: 288.1236; found: 288.1217.

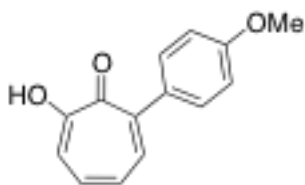
General Procedure For α -amino-2-aryl tropone Hydrolysis: α -amino-2-aryl tropone (1.0 eq) was dissolved in 1:1 EtOH:H₂O (2.0 M) to which was added 2 N KOH (20 eq). The reaction was heated to 100 °C and stirred for 16 h. The reaction was returned to room temperature and diluted with 15 % NaOH. The aqueous layer was washed with Et₂O (3 x) and CH_2Cl_2 (3 x) and then acidified to pH 2.0 and extracted with CH_2Cl_2 (3 x) washed with brine, dried over Na_2SO_4 , filtered, and concentrated *in vacuo*.



S14 α -phenyl tropolone 4a: 90 % yield; R_f = 0.52 (1:19 *i*PrOH: CH_2Cl_2); M_p = N/A; IR (KBr): ν : 3200-2800 broad, 2917, 2848, 1721, 1712, 1615, 1595, 1548, 1417, 1247, 737, 698. ^1H NMR (500 MHz, CD_2Cl_2) δ 7.60 (d, J = 9.9 Hz, 1H), 7.51 (d, J = 7.4 Hz, 2H), 7.46 (t, J = 14.8, 7.2, 7.6 Hz, 2H), 7.42-7.39 (m, 3H), 7.10 (t, J = 17.2, 7.7, 9.5 Hz, 1H). ^{13}C NMR (126 MHz, CD_2Cl_2) δ 171.9, 170.8, 141.1, 140.7, 139.5, 137.3, 129.8, 128.7, 128.6, 127.9, 122.0. HRMS (ESI) calcd for $\text{C}_{13}\text{H}_{11}\text{O}_2$ $[\text{M}+\text{H}]^+$: 199.0759; found: 199.0749.

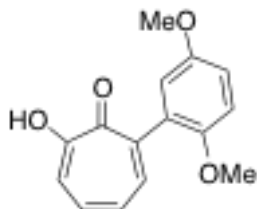


α -naphthyl tropolone 4b: 91 % yield; R_f = 0.52 (1:19 *i*PrOH: CH_2Cl_2); M_p = N/A; IR (KBr): ν : 3200-2800 broad, 3173, 3044, 2925, 1614, 1593, 1548, 1470, 1367, 1258, 1242, 1210, 800, 773, 689. ^1H NMR (500 MHz, CD_2Cl_2) δ 7.96 (d, J = 7.3 Hz, 2H), 7.61-7.50 (m, 6H), 7.44 (t, J = 14.0, 6.9, 7.1 Hz, 2H), 7.13-7.09 (m, 1H). ^{13}C NMR (126 MHz, CD_2Cl_2) δ 171.6, 170.8, 141.6, 138.6, 138.2, 137.2, 134.1, 131.5, 129.0, 128.9, 127.8, 127.0, 126.7, 126.5, 126.0, 125.9, 123.8. HRMS (ESI) calcd for $\text{C}_{17}\text{H}_{13}\text{O}_2$ $[\text{M}+\text{H}]^+$: 249.0916; found: 249.0928.

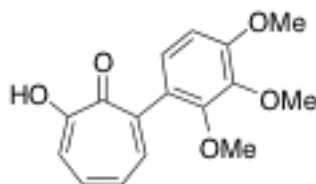


α -(4-methoxy-phenyl) tropolone 4c: 92 % yield; R_f = 0.52 (1:19 *i*PrOH: CH_2Cl_2); M_p = N/A; IR (KBr): ν : 3200-2800 broad, 3128, 3027, 1920, 1802, 1615, 1593, 1499, 1367, 1039, 802, 728. ^1H NMR (500 MHz, CD_2Cl_2) δ 7.49 (d, J = 10.0 Hz, 1H), 7.42-7.39 (m, 3H), 7.22 (dd, J = 7.4, 1.5, 1.5 Hz, 1H), 7.07-7.02 (m, 3H), 3.76 (s, 3H). ^{13}C NMR (126 MHz, CD_2Cl_2) δ 171.2, 170.9, 157.1, 141.4, 137.5, 136.5, 130.7, 130.1,

129.8, 127.4, 122.6, 121.0, 111.7, 56.1. HRMS (ESI) calcd for $C_{14}H_{13}O_3$ $[M+H]^+$: 229.0865; found: 229.0854.



α -(2,5-methoxy-phenyl) tropolone 4d: 89 % yield; R_f = 0.52 (1:19 *i*PrOH:CH₂Cl₂); M_p = N/A; IR (KBr): ν : 3200-2800 broad, 2930, 2832, 2002, 1925, 1797, 1615, 1595, 1548, 1496, 1398, 1201, 1044, 1024, 805, 728. ¹H NMR (500 MHz, CD₂Cl₂) δ 7.49 (d, J = 10 Hz, 1H), 7.39-7.37 (m, 2H), 7.07-7.03 (m, 1H), 6.97-6.92 (m, 2H), 6.82 (d, J = 2.7 Hz, 1H), 3.79 (s, 3H), 3.71 (s, 3H). ¹³C NMR (126 MHz, CD₂Cl₂) δ 171.1, 170.9, 154.1, 151.3, 141.3, 137.6, 136.3, 130.7, 127.4, 122.6, 116.7, 114.4, 112.9, 56.8, 56.2. HRMS (ESI) calcd for $C_{15}H_{15}O_4$ $[M+H]^+$: 259.0970; found: 259.0956.



α -(2,3,4-methoxy-phenyl) tropolone 4e: 89 % yield; R_f = 0.55 (1:19 *i*PrOH:CH₂Cl₂); M_p = N/A; IR (KBr): ν : 3200-2800 broad, 2994, 2938, 2837, 1992, 1920, 1713, 1614, 1596, 1408, 1301, 1108, 1046, 793, 735. ¹H NMR (500 MHz, CD₂Cl₂) δ 7.49 (d, J = 10 Hz, 1H), 7.40-7.36 (m, 2H), 7.07-7.01 (m, 1H), 6.93 (d, J = 8.6 Hz, 1H), 6.77 (d, J = 8.6 Hz, 1H), 3.89 (s, 3H), 3.89 (s, 3H), 3.74 (s, 3H). ¹³C NMR (126 MHz, CD₂Cl₂) δ 171.9, 170.4, 154.6, 151.8, 142.7, 141.4, 173.3, 136.8, 127.5, 127.4, 124.8, 122.2, 107.8, 61.4, 61.1, 56.5. HRMS (ESI) calcd for $C_{16}H_{17}O_5$ $[M+H]^+$: 289.1076; found: 289.1103.